Fault Tolerance of Semi-Active Seismic Isolation

Henri Gavin (A.M.), Cenk Alhan, Natasha Oka
Department of Civil and Environmental Engineering
Duke University
Durham, North Carolina 27708–0287

tel: 919–660–5201
fax: 919–660–5219
e-mail: hpgavin@duke.edu
URL: http://www.duke.edu/~hpgavin/
July 14, 2001

Abstract

A six story seismically isolated structure fitted with semi-active hydraulic devices is analyzed in order to study the effect of time delay in the devices and mass eccentricity in the super-structure on the lateral-torsional behavior. The computer program 3DBASIS, which allows the non linear dynamic analysis of three dimensional structures, is used in this work. Appropriate modifications were made to this program to incorporate the behavior of semi-active hydraulic devices. Three different types of base isolation systems were considered: (1) lead rubber bearings; (2) lead rubber bearings with supplemental viscous damping, and (3) lead rubber bearings with semi-active viscous damping.

A comparison of these three base isolation systems, considering both the effects of eccentricity in the structure and differential time lags in semi-active hydraulic devices are studied. The peak isolator shear, isolation drift, rotation and torsional moment are reported. Three major earthquake motion records, namely the El-Centro record of the 1940 Imperial Valley Earthquake, the Meloland record of the 1979 Imperial Valley Earthquake, and the Sylmar free field record of the 1994 Northridge Earthquake were used as inputs in the analyses.

Keywords: Base Isolation, Smart Damping, Vibration Control, Earthquake Engineering

INTRODUCTION

Seismic isolation is a highly successful method for protecting structures from earthquakes. The basic objectives in the seismic isolation of building structures are to protect the integrity of the structures and to prevent injury to the occupants and damage to the contents (Housner et al. 1997, Kelly 1997, Naeim and Kelly 1999, Skinner et al. 1993, Meirovitch and Stemple 1997). The compliant elastomeric bearings and frictional sliding mechanisms installed in the foundations of seismically isolated structures protect these structures from strong earthquakes through a reduction of stiffness and an increase in damping. The reduction of stiffness is intended to detune the structures fundamental period from the characteristic period of earthquake ground motions. Isolation bearings are designed to accommodate large displacement demands and to mobilize damping mechanisms, typically through material yielding of a lead column within the isolator. Elastomeric bearings are made by vulcanizing sheets of rubber to thin steel reinforcing plates, and are stiff in the vertical direction and flexible in the horizontal direction (Kelly 1997, Naeim and Kelly 1999). Because of this, under seismic loading, the bearing system isolates the building from the horizontal components of the ground movement. Friction pendulum bearings for seismic isolation were evaluated by Tyler (1977). A simple but efficient method of analysis was proposed for the dynamic analysis of the sliding isolation which is a highly non-linear dynamic problem (Wang et al. 1998). An experimental study was performed to evaluate the feasibility of a sliding isolation system equipped with uplift restraint devices for medium rise buildings subject to column uplift (Nagarajaiah et al. 1992).

Base isolation systems are being implemented in an increasing number of projects in highly seismic areas throughout the world (Hussain and Retamal 1994). The first base-isolated building in the United States was the Foothill Communities Law and Justice Center in San Bernardino County, CA in 1986 (Kelly, 1991). More recent examples of seismically isolated buildings include the USC University Hospital in Los Angeles, the Emergency Operations Center in Los Angeles, the U.S. Court of Appeals in San Francisco, and the San Bernardino County Medical Center (EERC 2001). Some examples of buildings constructed using

rubber bearing isolation system are the Salt Lake City and County building, the Rockwell International Headquarters in Seal Beach CA, the Long Beach Hospital in Long Beach CA, the State of California Justice Building in San Francisco, and the Government Office Building in Wellington, New Zealand.

During the 1994 Northridge earthquake, the seismic isolation system of the USC Hospital building reduced its response when compared to an equivalent fixed-base structure (Nagarajaiah et al. 1999). The peak roof acceleration was reduced to $0.21g$, only 50% of the peak ground acceleration. The bearings yielded and dissipated energy and the superstructure remained elastic. Experiments on two four-story buildings, one supported on high damping rubber isolation and the other on a fixed-base, were conducted by Moron et al. (1998) in Santiago, Chile. For the twenty-four earthquake records evaluated, the reduction in the maximum acceleration at the roof level for the isolated building, as compared to the fixed-base one, varied from 1 to 3.5, depending on the level of maximum ground acceleration and the characteristics of the earthquake motions. Other base isolated structures behaved as designed during the 1994 Northridge and 1995 Kobe earthquakes (Kelly 1991, DIS 2001). On the other hand, protection of seismically isolated structures from strong, long-period velocity pulses is more challenging. A study by Heaton et al. (1995) showed that a base isolated building subjected to a near-field $M_w 7.0$ blind thrust earthquake could result in large isolator drifts (in excess of 50 cm) even when damped at 25% critical damping. Large displacements at the isolation interface during a strong earthquake can lead to buckling or rupture of the isolation bearings (Nagarajaiah and Ferrell 2000). Although, large levels of damping reduce isolator displacements in the fundamental mode, they impart forces into the structure which increase structural accelerations and deformations in higher modes, and can increase inter-story displacements (Kelly 1999). To address the need for high damping to limit the isolation drift and low damping to improve the isolation effectiveness at high frequencies, multiple controllable damping (semi-active) systems have been proposed (Gavin and Doke 1999, Symans and Constantinou 1999, Yang et al. 2000, Carlson and Spencer 1996, Johnson et al. 1998, Patten et al. 1998, Symans and Constantinou 1997a, 1997b). Semi-active control systems were first proposed in the 1920's, as shock absorbers which utilized an elastically supported mass to activate hydraulic valving. No external power or a solenoid valve was necessary to direct the hydraulic flow within the damper (Karnopp et al. 1974, 1975). Semi-active control systems are a class of active control systems for which the external energy requirements are insignificant. Typically semi-active devices can not add mechanical energy to the structural system, therefore bounded-input, bounded-output stability is guaranteed and they are often viewed as controllable passive systems. Semi-active control systems take advantage of the reliability of passive control systems, while providing the adaptability of active control systems. Semi-active systems require only a small amount of external power for operation and utilize the motion of the structure to develop the control forces (Symans and Constantinou 1999).

Semi-active devices can be categorized into the following kinds (Kurata 1999).

- *Controllable Fluid Damper*: These encompass devices which utilize electrorheological materials and magnetorheological materials (Ehrgott and Masri 1993, Gavin 1996, Markis, Hills, Burton and Jordan 1995, Spencer, Dyke and Sain 1996, and Carlson and Spencer 1996). These materials have the ability to change from free flowing viscous fluids to a semi-solid state in a matter of milli-seconds when exposed to an electric or a magnetic field. These devices are mechanically reliable, since they do not contain any moving parts.

- *Controllable Friction Damper*: These dampers utilize the force generated by surface friction to dissipate energy. Dowdell and Cherry proposed a variable slip force friction damper and an "ON-OFF" friction damper. Hirai, Naruse and Abiru (1996) investigated a variable friction damper utilizing piezoelectric actuators. Akbay and Aktan (1990) proposed a friction slip brace. A study by Feng (1993) investigates into a hybrid isolation system - a frictional controllable sliding system. This hybrid system was developed using friction controllable bearings. It is shown that this type of system is effective for earthquakes with a broad range of intensity, compared to its conventional passive counterparts.

- *Hydraulic Damper*: Fluid viscous dampers have found numerous applications in the shock vibration isolation of aerospace and defense systems. The earliest well documented use of large fluid dampers was by the military to reduce the recoil of large canons. Karnopp (1990) introduced semi-active isolators using the skyhook damper scheme. Practical applications of sky-hook dampers, namely extreme isolation for delicate manufacturing operations against seismic input and the automotive suspensions are discussed by Karnopp (1995). Patten, Kuehn and Lee (1998), provided a primer on

the important physical characteristics of a hydraulic semi-active vibration absorber. An important benefit of the fluid viscous dampers is that they are especially effective in minimizing the forces acting on building columns. They reduce the drifts and shear forces which are in phase with column bending moments.

The development and evaluation of semi-active control systems for applications in structural control is receiving particular attention (Symans and Constantinou 1999). Numerical simulations, vibration tests and semi-active vibration suppression experiments of a 10-bay truss bridge with ER fluid dampers are performed by Onoda et al. (1997). Gavin and Hanson (1998) showed that adaptive base isolation systems using electrorheological materials in viscous damping walls can reduce absolute velocities in upper stories as well as deflections in the isolation system. Seismic testing of a multi-story building structure with a semi-active fluid damper control system was performed by Symans and Constantinou (1997a). The semi-active dampers were installed in the lateral bracing of the structure and the mechanical properties of the dampers were modified according to control algorithms which utilized the measured response of the structure. An intelligent base-isolation system, comprised of low damping isolation bearings and controllable fluid dampers is studied by Johnson et al. (1998). In an other study, Symans and Constantinou (1997b) discussed the development, experimental testing and analytical modeling of an intelligent seismic control system. These studies demonstrate the potential of semi-active damping systems, but do not consider the possibility of asymmetry in the buildings or relative time delay between the semi-active devices. While many previous studies have shown the benefits of semi-active control in planar structures, the possibility of mis-timed devices due to technical problems may result in high torsional response. This increase in high torsional response is typically compounded by the effects of significant mass eccentricity. Very few analytical studies have been reported on the seismic base isolation of 3D building models (Jangid and Datta 1995). Lee (1980) has shown that base isolation reduces the structural torque even if the structural eccentricity is large. Pan and Kelly (1983) studied the effect of eccentricity on the elastic response of a rigid mass supported on a base isolator. Nagarajaiah et al. (1991, 1993) studied the response of a 3D base isolated building with bi-axial hysteretic isolators. Jangid and Datta (1992, 1993, 1994, 1995) conducted parametric studies on the response behavior of a torsionally coupled base isolation system. Additionally, it is widely recognized that time delays exist in active control systems and must be considered to ensure dynamic stability (McGreevy et al. 1988, Soong 1990, Symans and Constantinou 1997a).

In this paper, the effects of time delay in the semi-active devices and the eccentricity in the mass of the super-structure are studied. A comparison between three base isolation systems is presented: (1) lead rubber bearings (LRB); (2) lead rubber bearings with supplemental viscous damping (LRB-VD), and (3) lead rubber bearings with semi-active viscous damping (LRB-SAVD). Three major earthquake motion records, namely the El-Centro record of the 1940 Imperial Valley Earthquake, the Meloland record of the 1979 Imperial Valley Earthquake, and the Sylmar free field record of the 1994 Northridge Earthquake, were used as inputs in the analyses. The El Centro record is selected as a moderate type of earthquake, while Meloland and Sylmar records represent the pulse-like type of earthquakes. This study addresses the robustness of semi-active base isolation systems with respect to relative time delays among the devices.

CONTROL RULE DEVELOPMENT AND DEVICE PLACEMENT

Consider a base isolated building with controllable hydraulic devices as shown in Figure 1. The displacement z is the displacement of the ground with respect to an inertial reference frame. The displacements of the degrees of freedom with respect to the ground are $x_1, \cdots, x_7$. The control objective is to suppress the absolute motion of the building and to thereby reduce the dynamic shear forces carried by the structure. Ideally, this can be achieved by means of a fictitious passive damper which imparts a force to the building foundation proportional to the absolute velocity $\dot{z} + \dot{x}_1$ of the base as illustrated in Figure 1. The behavior of this fictitious damper can be mimicked by a semi-active control device placed as shown in Figure 1. The device will have high damping (ON) when the force in the device opposes the velocity $(\dot{x}_1 + \dot{z})$ and will have low damping (OFF) otherwise (Karnopp 1974).

This physically motivated control strategy can be mathematically derived as follows. The equations

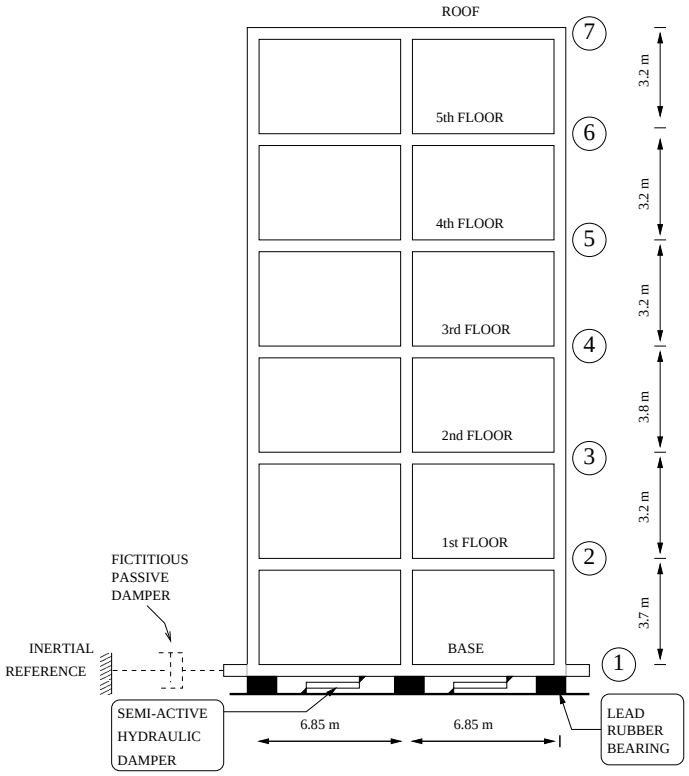

Figure 1: Base isolated structure with controllable hydraulic device

of motion of a base excited structure are given by

$$\mathbf{M}(\ddot{\mathbf{x}} + \mathbf{H}\ddot{\mathbf{z}}) + \mathbf{r}(\mathbf{x}, \dot{\mathbf{x}}) + \sum_{n=1}^{N} \mathbf{b}_n f_n(\mathbf{b}_n^T \mathbf{x}, \mathbf{b}_n^T \dot{\mathbf{x}}, u_n) = \mathbf{0} \tag{1}$$

where $\mathbf{b}$ is the control input vector and depends on the placement of the n^{th} device. $\mathbf{H}$ is a boolean earthquake input matrix, $\ddot{\mathbf{z}}$ are the two orthogonal components of horizontal ground acceleration, $\mathbf{r}(\mathbf{x}, \dot{\mathbf{x}})$ are generalized nonlinear restoring forces, and $\mathbf{M}$ is a positive definite mass matrix.

The total energy of the system is given by

$$V(t) = W(\mathbf{x}, \dot{\mathbf{x}}) + \frac{1}{2}(\dot{\mathbf{x}} + \mathbf{H}\dot{\mathbf{z}})^T \mathbf{M}(\dot{\mathbf{x}} + \mathbf{H}\dot{\mathbf{z}}) \tag{2}$$

where $(\dot{\mathbf{x}} + \mathbf{H}\dot{\mathbf{z}})^T \mathbf{M}(\dot{\mathbf{x}} + \mathbf{H}\dot{\mathbf{z}})$ is the absolute kinetic energy of the system and $\mathbf{r}(\mathbf{x}, \dot{\mathbf{x}})$ is the gradient of the potential energy function $W(\mathbf{x}, \dot{\mathbf{x}})$. Following Lyapunov's direct method (Khalil 1996), the objective of the control is to minimize the internal energy by forcing the rate of change of the internal energy to be as negative as possible. The rate of change of the internal energy is

$$\dot{V}(t) = -\dot{\mathbf{z}}^T \mathbf{H}^T \mathbf{r} - \sum_{n=1}^{N} [(\dot{\mathbf{x}} + \mathbf{H}\dot{\mathbf{z}})^T \mathbf{b}_n f_n(\mathbf{b}_n^T \mathbf{x}, \mathbf{b}_\mathbf{n}^\mathbf{T} \dot{\mathbf{x}}, \mathbf{u_n})] \tag{3}$$

The only terms that can be controlled in equation (3) are the terms in square brackets. In order to make $\dot{V}(t)$ as negative as possible, a device's force should be made large whenever the quantity in the square bracket is positive, otherwise the device force should be small. The vectors $\mathbf{b}_n$ define the placement of the devices. For a device connecting degrees of freedom "i" to the base, $b_i = 1$ and all other elements of $\mathbf{b}$ are zero. If the device connects degree of freedom "i" with the degree of freedom "j", then $b_i = 1$, $b_j = -1$,

and all other elements of $\mathbf{b}$ are zero. Also note that controllable damping devices satisfy a sector-bounded passivity constraint: $\mathbf{b}^T\dot{\mathbf{x}}f(\mathbf{b}^T\mathbf{x}, \mathbf{b}^T\dot{\mathbf{x}}) > 0$ unconditionally. Therefore, if $b_{i,j} = \pm 1$ then

$$(\dot{\mathbf{x}} + \mathbf{H}\dot{\mathbf{z}})^T\mathbf{b} = \dot{x}_i - \dot{x}_j = \mathbf{b}^T\dot{\mathbf{x}} \tag{4}$$

and if $b_i = 1$ only

$$(\dot{\mathbf{x}} + \mathbf{H}\dot{\mathbf{z}})^T\mathbf{b} = \dot{x}_i + \dot{z} \neq \mathbf{b}^T\dot{\mathbf{x}} \tag{5}$$

Therefore, if one end of the device is not attached to the moving ground, the term in the square bracket is always positive. Such a device placement requires the device to be "ON" always, which defeats the very purpose of a controllable device. Thus, for this particular control rule, the controllable device is placed between the foundation and the ground (Gavin and Doke 1999, Gavin 2001). The control rule reduces to turning the n^{th} semi-active device "ON" to maximize its damping when $f \cdot V_a > 0$, where V_a is the absolute velocity of the structure-side of the device. The control decision is based only on the motion and force of the device, and no centralized control computation is needed.

DESIGN AND MODELING OF THE SEMI-ACTIVE HYDRAULIC DEVICE

The controllable damping device modeled in this study compromises a hydraulic cylinder with a controllable by-pass valve and can be fashioned from a conventional damper with provision for fast modulation of the damping coefficient. The device is termed 'semi-active', because the power required to perform the necessary modulation in forces is generated by the motion of the structure itself.

Consider a fluidic device as shown in Figure 2. The control device illustrated here essentially consists of a cylinder, a piston, and a valve. The flow of fluid is controlled by means of a valve, with a variable valve coefficient $c_v(v)$. The area of the piston is A_p, the pressure differential across the two chambers is $p_2 - p_1$ and the device contains a volume of fluid V_T where $V_T = V_1 + V_2$. The diameter of the bore and that of the rod are D_b and D_r respectively. The force, f, in the piston rod is $A_p(p_2 - p_1)$. Assuming incompressible

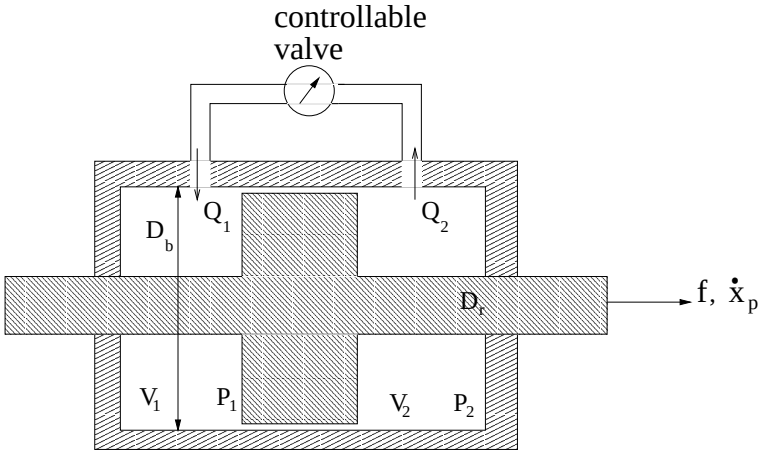

Figure 2: Details of hydraulic device

flow in the valve, $Q_1 = Q_2 = Q$, and approximating a linear pressure-flow relationship for the controllable valve, $(p_2 - p_1) = c_v^*(v)Q$. Considering fluid compressibility within the chambers 1 and 2, $\dot{p}_1 V_1 = -\beta\dot{V}_1$ and $\dot{p}_2 V_2 = -\beta\dot{V}_2$, where β is the bulk modulus of the hydraulic fluid which can range from 80 to 200 kN/cm^2 and where we apply the conventions that $\dot{V} > 0$ means volumetric expansion and $\dot{p} > 0$ means increasing hydrostatic compression. In chamber 1, $\dot{V}_1 = -Q_1 + A_p\dot{x}_p$ and in chamber 2, $\dot{V}_2 = Q_2 - A_p\dot{x}_p$. Substituting the valve equation, the equilibrium equation and the compressibility equations, we obtain (Patten et al. 1998, Gavin and Doke 1999),

$$\dot{p}_2 = -\frac{\beta}{V_2}\frac{f}{A_p c_v^*(v)} + \frac{\beta}{V_2}A_p\dot{x}_p, \tag{6}$$

and

$$-\dot{p}_1 = -\frac{\beta}{V_1}\frac{f}{A_p c_v^*(v)} + \frac{\beta}{V_1}A_p\dot{x}_p. \tag{7}$$

Adding these equations,

$$\dot{p}_2 - \dot{p}_1 = -\frac{\beta}{A_p c_v^*(v)}\left(\frac{1}{V_1}+\frac{1}{V_2}\right)f + \beta A_p\left(\frac{1}{V_1}+\frac{1}{V_2}\right)\dot{x}_p, \tag{8}$$

and the equation for the damper force, including compressibility and viscous effects, is

$$\dot{f} = \frac{k_d}{c_v(v)}f + k_d\dot{x}_p, \tag{9}$$

where

$$k_d = \frac{4\beta A_p^2}{V_T}, \tag{10}$$

is the hydraulic stiffness of the device. Considering elastic properties of the built-up device, the overall device stiffness k_d is less than the hydraulic stiffness. The device valve constant c_v is defined as $c_v = c_v^* A_p^2$. Here, f, k_d, and c_v are the force, stiffness and damping in the device respectively and $c_v(v)$ is the only term that can be controlled, by the valve-opening variable, v. This valve coefficient $c_v(v)$ is assumed to vary linearly with the valve variable v,

$$c_v(v) = (1-v)c_{min} + vc_{max}. \tag{11}$$

The constants c_{min} and c_{max} are the damping coefficients when the device is "OFF" and "ON" respectively, and, the valve has a first order delay modeled by

$$\dot{v} = \frac{1}{T_v}(u - v) \tag{12}$$

where T_v is the valve time constant and u is the control input which depends on the control rule. For the particular control rule considered in this study u is bounded by $0 \le u \le 1$ and is given by

$$u = H(f \cdot V_a) \tag{13}$$

where V_a is the absolute velocity of the structure side of the device with respect to an inertial reference frame and $H(\cdot)$ is the Heaviside step function.

Appropriate values for the device parameters, c_{min}, c_{max}, and k_d are determined through iterative time history analyses of the semi-active isolation system. To design the cylinder and piston arrangement we need to find a suitable bore diameter D_b, rod diameter D_r , piston stroke, S, and fluid volume, V_T. The area of the piston is determined by the force requirement, F_{max},

$$A_p = \frac{F_{max}}{P_{max}} = \frac{\pi}{4}({D_b}^2 - {D_r}^2), \tag{14}$$

where P_{max} is the maximum pressure which is typically equal to 2 to 5 KN/cm^2 for the device under consideration. The diameter of the rod should be such that

$$0.5\sigma_y\pi\frac{{D_r}^2}{4} > F_{max} \tag{15}$$

to prevent yielding of the piston rod where σ_y is the yield stress and is approximately equal to 40 ksi. Substituting D_r from equation 15 into equation 14, we have

$${D_b}^2 > \frac{4}{\pi}A_p + {D_r}^2 \tag{16}$$

The stroke of the device should be long enough to accommodate the displacement demand D_{max}. Thus the stroke should be such that $S > 2D_{max}$. The volume of fluid V_T is given by $V_T = A_p S$.

EXTENSION TO 3D BASIS

The program 3DBASIS (Nagarajaiah, 1991) computes the non linear dynamic response of three dimensional base isolated structures and is widely used for structural engineering research and design. Buildings analyzed by 3DBASIS have three degrees of freedom per story: two translations and one rotation. Models for a number of isolation systems, including elastomeric bearing isolation systems and sliding isolation systems with re-centering devices are implemented in this program and can be combined to model an isolation system completely. Additionally, the program takes into account the lateral-torsional interaction of forces in both horizontal directions, and the biaxial hysteretic behavior of each individual isolator.

In this study we implement a semi-active hydraulic device in parallel with a hysteretic lead-rubber bearing isolation system. The device is modeled as an additional new isolation element. A fourth order Runge-Kutta method (Butcher 1987) is employed for the purposes of solution of the first order differential equations for the isolators and the semi-active device.

The device acts as a uniaxial element. The control rule requires the absolute velocity as an input which can be obtained via on-line integration of acceleration (Gavin 1998, 2001). In this study, the absolute velocity of the earthquake ground motion is pre-computed.

SIMULATIONS

In this section, we present the simulation results for a typical structure subjected to different earthquake input motions. Response of the same structure with three different types of base isolation systems, namely; lead rubber bearings, lead rubber bearings with supplemental viscous damping, and lead rubber bearings with semi-active viscous damping.

Description of the Model

A six story reinforced concrete structure as shown in Figure 1 and Figure 3 is considered for the purposes of the simulations. This structure is similar to the one used by Nagarajaiah et al. (1998). The total weight of the structure is 2205 tons. The fixed base frequencies of the structure for the first three modes are 1.147, 1.202 and 2.503 Hz. The rigid body isolation period (T_b) is 1.65 seconds. Damping of 5% of critical is assumed for the superstructure in all the modes.

In the lead-rubber bearing isolation system model, the post yielding to pre yielding stiffness ratio is 0.154, the yield force is 75.8 kN, and the yield displacement is 7.00 mm.

Four hydraulic devices, two in each of the orthogonal directions as shown in Figure 3, are installed in parallel with 18 lead rubber bearings, which are placed under the columns. The stiffness,k_d, of the hydraulic devices are 300000 kN/m and c_{max} and c_{min} are 3000 kN/m/sec and 300 kN/m/sec respectively. The relative mis-timing of the semi-active devices is given by dimensionless quantities α and β, where α is the ratio between the time constants of the devices in the NS direction, given by T_1/T_2, and β is the ratio between the time constants of the devices in the EW direction, given by T_3/T_4, and where T_1, T_2, T_3 and T_4 are the time constants of device 1, 2, 3, and 4 respectively. The response of the structure is simulated for values of α and β equal to 1, 2, 5, and 10. The results only those corresponding to variations in α are given in this paper. The results corresponding to variations in β are qualitatively similar to the results corresponding to variations in α (Oka 1998).

Earthquake Data

The three models mentioned above were each subjected to 3 different earthquake input motions in both the orthogonal directions:

1. The May 18, 1940 Imperial valley earthquake recorded at El Centro site Imperial Valley irrigation district. The peak acceleration in NS and EW directions are 0.34 g and 0.21 g, respectively.

2. The October 15, 1979 Imperial valley earthquake recorded at Meloland station. The peak acceleration in NS and EW directions are 0.31 g and 0.29 g, respectively.

3. The January 17, 1994 Northridge earthquake recorded at Sylmar Hospital free field station. The peak acceleration in NS and EW directions are 0.8 g and 0.6 g, respectively.

Eccentricity Norm

In order to quantify the mass eccentricity of the structure let us define an eccentricity norm as

$$e = \sqrt{(e_x^2 + e_y^2)} \tag{17}$$

where e_x and e_y are the mass eccentricities of the superstructure in the X and Y direction with respect to the center of mass of the base, which coincides with the shear center.

The response of the structure is simulated with different eccentricity norms. The eccentricities in both the orthogonal directions are varied from zero to one-fourth of the length of the structure in the respective direction. For this model problem e_x and e_y were varied from 0m to 4.5m and 0m to 3.4m respectively.

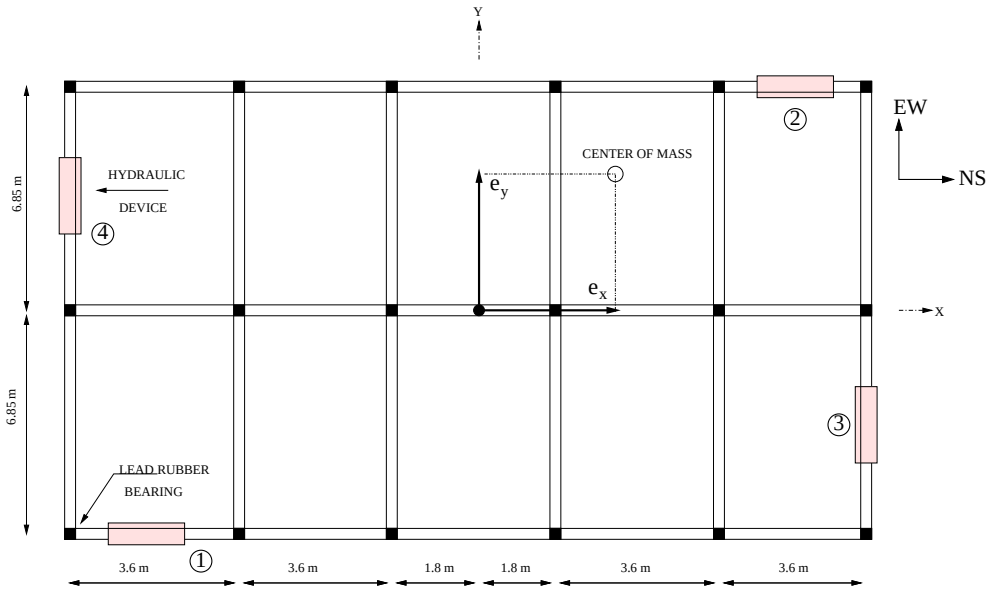

Figure 3: Six story structure : Plan

RESULTS

Our aim is to control the isolation damping in order to reduce the isolator drift without increasing the base shear. Peak isolation drift, peak base shear, peak base rotation, and peak torsional moment are plotted against the eccentricity norm for all systems: the base isolation system (lead rubber bearings only) and the systems with the semi-active hydraulic devices (the controlled valve and the closed valve cases) for each earthquake.

El-Centro Record of the Imperial Valley earthquake

The maximum isolation drift, maximum base shears, maximum base rotation, and maximum torsional moment responses for the El-Centro record are tabulated in Table 1. Comparison of the isolation drift, rotation, base shears, and torsional moment, for different eccentricities in the superstructure, are given in Figure 4 for the lead rubber bearing system (LRB), the semi-active (LRB-SAVD) system with variation in α, and the semi-active system with closed valves (LRB-VD) for the El Centro record.

For the El Centro ground motions, the LRB-SAVD system results in isolation drifts and rotations that are 20 to 40 percent smaller than both the LRB and LRB-VD cases. The LRB-SAVD system does not increase the base shear in the NS direction but increases the base shear by 5 to 30 percent in the EW direction. However, the maximum torsional moment for both the LRB-SAVD and LRB-VD has increased by about 500-700 ton-meters as compared to the LRB system. The eccentricity does not have a significant

effect on the isolation drift, base shear, and the base rotation for the system with the semi-active device. However, the torsional moments increase by 60 percent (800 ton-meters) as the eccentricity increases. The effect of the time delay is significant only in the base shear response in the NS direction.

Response		LRB		LRB-SAVD		LRB-VD	
		$e = 0$m	$e = 5.64$m	$e = 0$m	$e = 5.64$m	$e = 0$m	$e = 5.64$m
Max. base disp. (meters)	N-S	0.081	0.091	0.046	0.036	0.060	0.052
	E-W	0.073	0.073	0.043	0.046	0.062	0.062
Max. base shear (tons)	N-S	359	327	352	335	342	325
	E-W	305	267	325	269	254	227
Max. base rotation	-	0.00084	0.01038	0.00121	0.00407	0.00187	0.00451
Max. Z moment (ton-meters)	-	573	1585	1274	2017	1107	1638

Table 1: Comparison of response of Base isolation system and semi-active device for El Centro

Meloland Record of the Imperial Valley earthquake

The maximum isolation drift, maximum base shears, maximum base rotation, and maximum torsional moment for the Meloland record are tabulated in Table 2. Comparison of the isolation drift, rotation, base shears, and torsional moment responses, for different eccentricities in the superstructure, are given in Figure 5 for the LRB system, the LRB-SAVD system with variation in α, and the LRB-VD system for the Meloland record.

Response		LRB		LRB-SAVD		LRB-VD	
		$e = 0$m	$e = 5.64$m	$e = 0$m	$e = 5.64$m	$e = 0$m	$e = 5.64$m
Max. base disp. (meters)	N-S	0.213	0.211	0.085	0.081	0.103	0.150
	E-W	0.383	0.273	0.129	0.114	0.092	0.129
Max. base shear (tons)	N-S	683	718	535	480	486	453
	E-W	1271	846	684	596	732	599
Max. base rotation	-	0.00324	0.04295	0.00468	0.00991	0.00546	0.01191
Max. Z moment (ton-meters)	-	840	4767	1308	2017	1447	2463

Table 2: Comparison of response of Base isolation system and semi-active device for Meloland

The LRB-SAVD system reduces the isolation drift by 55 percent (12 cm) in the NS direction and 60 percent (16 cm) in the EW direction as compared to the LRB system, and by 20 percent (2 cm) in the NS direction and 10 percent (2 cm) in the EW direction as compared to the LRB-VD system. The LRB-SAVD system reduces the base shear by 20 percent in the NS direction and 35 to 45 percent (200 to 550 tons) in the EW direction as compared to the LRB system.

As compared to the LRB-VD system, the LRB-SAVD system increases the base shear by 15 percent (60 tons) in the NS direction but decreases it by 9 percent (60 tons) in the EW direction.

In regards to the torsional moments and rotations, the LRB-SAVD and LRB-VD systems behave almost identically. The torsional response increases monotonically with mass eccentricity, while the isolation drift and base shear in the EW direction decrease monotonically with the mass eccentricity. The LRB system is much more sensitive to the mass eccentricity than the LRB-SAVD and LRB-VD systems. As in the El Centro response, the effect of time delay is not pronounced.

Sylmar Record of the Northridge earthquake

The maximum isolation drift, maximum base shears, maximum base rotation, and maximum torsional moment for the Sylmar record are tabulated in Table 3. Comparison of the isolation drift, rotation, base

shears, and torsional moment, for different eccentricities in the superstructure, are given in Figure 6 for the LRB system, the LRB-SAVD system with variation in α and the LRB-VD system for the Sylmar record.

Response		LRB		LRB-SAVD		LRB-VD	
		$e = 0$m	$e = 5.64$m	$e = 0$m	$e = 5.64$m	$e = 0$m	$e = 5.64$m
Max. base disp. (meters)	N-S	0.528	0.334	0.233	0.224	0.249	0.241
	E-W	0.441	0.281	0.132	0.126	0.143	0.135
Max. base shear (tons)	N-S	1650	1404	1087	1082	1097	1100
	E-W	1117	918	713	656	686	596
Max. base rotation	-	0.00335	0.01721	0.00275	0.00615	0.00289	0.00486
Max. Z moment (ton-meters)	-	825	3266	2130	3810	2189	3660

Table 3: Comparison of response of LRB system and LRB-SAVD device for Sylmar

The LRB-SAVD system reduces the isolation drift by 50 to 60 percent (23 to 31 cm) in the NS direction and by 40 to 60 percent in the EW direction as compared to the LRB system. As compared to LRB-VD system, the LRB-SAVD system reduces the isolation drift by 10 percent (2cm).

The base shear for the LRB-SAVD and the LRB-VD systems are essentially the same, and are 20 to 30 percent (300 to 550 tons) smaller than those for the LRB system in the NS direction. In the EW direction, the LRB-SAVD and LRB-VD systems reduce the base shear by 10 to 35 percent (70 to 400 tons). The torsional moments for all these systems are essentially the same, whereas the torsional rotation for the LRB-SAVD and LRB-VD systems are 70 percent smaller than those of the LRB system. Again, the torsional response increases monotonically with the mass eccentricity. The NS response for the LRB case decreases monotonically with the mass eccentricity. The effect of time delay in the LRB-SAVD system is insignificant except for the torsional moment.

For all the earthquakes it is observed that unmatched time delays do not appear to degrade the system behavior. Also, the response of the structure installed with semi-active devices seems to more or less constant with increases in the mass eccentricity.

It is interesting to note that the benefits of the LRB-SAVD system are clearer for the Meloland and Sylmar records than for the El Centro record. The basic difference between these two earthquakes and El-Centro is that they contain a large velocity pulse. Thus, the semi-active damping system described in this paper appears to be well-suited to earthquakes that have a large velocity pulse.

DIMENSIONS OF THE HYDRAULIC DEVICE

We design the hydraulic device using the maximum force in the device, F_{max}, maximum displacement of the device, D_{max}, and maximum velocity of the device, V_{max} as computed in the dynamic simulations, in which c_{max} and c_{min} are 3000 kN/m/sec and 300 kN/m/sec respectively. F_{max}, V_{max}, and D_{max} are calculated as 92.71, 235.7, 375.2 tons ; 0.25, 0.60, 1.1 m/s ; and 5.4, 16.94, 24.67 cm for El Centro, Meloland and Sylmar earthquake records respectively. For a F_{max} range of 90 to 375 tons, a D_{max} range of 5 to 25 centimeters and a maximum velocity range of 0.25 to 1.1 m/s, and assuming a maximum fluid pressure of 3.6 kN/cm^2, a device with a rod diameter of 18.5 centimeters, bore diameter of 40.5 centimeters and a stroke of 0.5 meters is found to provide the target stiffness, k_d, of 300000 kN/m that was used in the analysis.

CONCLUSIONS

A non linear dynamic analysis of a structure fitted with a semi-active hydraulic device was performed using a program 3-D BASIS. The analysis was carried out on three different earthquake records. The results showed that semi-active hydraulic devices are capable of controlling the response of the structure especially in case of earthquake ground motions with a large velocity pulse. The semi-active hydraulic device performs better than the conventional base isolated system especially for the earthquakes with the large pulses.

For all the earthquakes, as the mass eccentricity increases, both the torsional moment and the base rotation, increase. However, mis-matched time-lags in the devices do not cause a significant increase in the torsional response. Semi-active control systems appear to be very robust to relative time delays between the devices. Even for the worst cases considered, where the ratio of the time constants between the devices in the same direction was 10, there was no significant increase due to the time-lag, neither in the torsional moments and base rotations, nor in the base shear and isolation drifts.

In the case of the moderate El Centro earthquake, there was a moderate increase in the base shear and the torsional moment in the system where semi-active devices are used as compared to the system where conventional base isolation is used.

In future work various control rules and magnetorheological fluid device models will be implemented.

ACKNOWLEDGEMENTS

This material is based on work supported by the National Science Foundation under Award No. CMS-9900193. Any opinions, findings, and conclusions or recommendations expressed in this publication are those of the authors and do not necessarily reflect the views of the sponsors.

APPENDIX. REFERENCES

1. Akbay, Z. and Aktan, H.M., (1990), "Intelligent energy dissipation devices," *Proc. 4th U.S. Nat. Conf. on Earthquake Engineering,* Vol. 3, pp. 427-435.

2. Butcher, J.C., (1987), "The numerical analysis of ordinary differential equations," *John Wiley and Sons.*

3. Carlson, J.D. and Spencer Jr., B.F., (1996), "Magnetorheological fluid dampers for semi-active seismic protection," *Proc. 3rd Int. Conf. on Motion and Vibration Control,* pp. 35-40.

4. Dynamic Isolation Systems (DIS), (2001), "Kobe Earthquake: effectiveness of seismic isolation proven again"/ *www.dis-inc.com*

5. EERC, UC Berkeley, (2001), "Seismically-Isolated Buildings in the United States," *http:// nisee.ce.berkeley.edu/prosys/usbldgs.html*

6. Ehrgott, R.C. and Masri, F., (1993), "Structural control applications of an electrorheological device," *Proc. Int. Workshop on Structural Control,* pp. 115-129.

7. Feng, M.Q., Shiozuka, M., and Fuji, S., (1993), "Friction controllable sliding isolated systems," *Journal of Engineering Mechanics,* vol 199, no. 9, pp 1845–1864.

8. Feng, M.Q., (1993), "Application of hybrid sliding isolation system to buildings," *Journal of Engineering Mechanics,* 119:2090-2108.

9. Gavin, H.P., Hanson, R.D., and McClamroch, N.H., (1996), "Control of structures using electrorehological dampers," *Proc. 11th World Conf. on Earthquake Engineering.*

10. Gavin, H.P. and N.S., Doke, (1999), "Resonance suppression through variable stiffness and damping mechanisms," *Proc. SPIE, 6th Annual Int. Symposium on Smart Structures and Materials.*

11. Gavin, H.P., (2001), "Control of seismically excited vibration using electrorehological materials and Lyapunov methods," *IEEE Transactions on Control Systems Technology,* 9(1): 27-36.

12. Gavin, H.P., Morales, R., Reilly, K., (1998), "Drift-free integrators," *Review of Scientific Instruments,* 69(5): 2171-2175.

13. Gavin, H.P. and R.D. Hanson., (1998), "Seismic protection using ER damping walls," *Proc. of the second world conference on structural control,* Vol 2, pp. 1183-1188.

14. Heaton, T.H., Hall, J.F., Wald, D.J., Halling, M.W., (1995), "Response of high-rise and base-isolated buildings to a hypothetical M_w7.0 blind trust earthquake," *Science,* 267:206-211.

15. Hirai, J., Naruse, M., and Abiru, H., (1996), "Structural control with variable friction damper for seismic response," *Proc. 11th World Conf. on Earthquake Engineering,*.

16. Housner, G.W., Bergman, L.A., Caughey, T.K., Chassiakos, A.G., Masri, S.F., Skelton, R.E., Soong, T.T., Spencer, B.F., and Yao, J.T.P., (1997), "Structural control: past, present and future," *Journal of Engineering Mechanics,* 123(9):897-971.

17. Hussain, S.M. and E. Retamal, (1994), "A hybrid seismic isolation system - isolators with supplemental viscous dampers," *Proceedings of First World Conference on Structural Control*, Los Angeles, California, USA, volume 3, pages (FA2-53)-(FA2-62).

18. Jangid, R.S and T.K. Datta, (1992), "Seismic behavior of torsionally coupled base isolated structure," *European Earthquake Engineering*, 3(92): 2-13.

19. Jangid, R.S and T.K. Datta, (1993), "Seismic response of a torsionally coupled system with a sliding support," *Journal of Struct. Build. Inst. Civ. Engrs.*, 99: 271-280.

20. Jangid, R.S and T.K. Datta, (1994), "Nonlinear response of torsionally coupled base isolated structure," *Journal of Structural Engineering*, 120: 1-22.

21. Jangid, R.S and T.K. Datta, (1995), "Performance of base isolation systems for asymmetric building subject to random excitation," *Engineering Structures*, 17(6): 443-454.

22. Johnson, E.A., Ramallo, J.C., Spencer, B.F., and Sain, M.K., (1998), "Intelligent base isolation systems," *Proc. of the second world conference on structural control,* Vol 1, pp. 367-376.

23. Karnopp, D., Crosby, M.J., and Harwood, R.A., (1974), " Vibration control using semi-active force generators," *ASME Journal of Engineering for Industry*, 96(2): 619-626.

24. Karnopp, D. and R., Allen, (1975), " Semi-active control of multi-mode vibratory systems using the ILSM concept," *ASME Journal of Engineering for Industry*, 98(3): 914-918.

25. Kelly, J.M., (1991), "Base isolation: origins and development," *EERC News,* 12(1).

26. Kelly, J. M., (1997), "Earthquake-Resistant Design With Rubber," *Springer Verlag.*, 2nd edition.

27. Kelly, J.M., (1999), "The role of damping in seismic isolation," *Earthquake Engineering and Structural Dynamics,* 28:3-20.

28. Khalil, H.K., (1996), "Nonlinear systems," *Prentice Hall* 2nd edition.

29. Kurata, N., Kobori, T., Takahashi, M., Niwa, N., and Midorikawa, H., (1999), "Actual seismic response controlled building with semi-active damper system," *Earthquake Engineering and Structural Dynamics,* 28:1427-1447.

30. Markis, N., Hills, D., Burton, S., Jordan, M., (1995), "Electrorheological fluid dampers for seismic protection of structures," *Proc. SPIE Conf. on Smart Structures and Materials,* pp. 184-194.

31. McGreevy, s., Soong, T.T., Reinhorn, A.M., (1988), "An experimental study of time delay compensation in active structural control," *Proc. 6th int. modal analaysis conf.,* vol 1., pp. 733-739.

32. Meirovitch, L.and T. J. Stemple, (1997), "Nonlinear control of structures in earthquakes", *Journal of Engineering Mechanics,* 123(10):1090-1095.

33. Moroni, M.O., Sarrazin, M., Boroschek, R., (1998), "Experiments on a base-isolated building in Santiago, Chile," *Engineering Structures,* 20(8):720-725.

34. Naeim, F. and J.M., Kelly, (1999), "Design of Seismic Isolated Structures : From Theory to Practice," *John Wiley and Sons.*

35. Nagarajaiah, S., Reinhorn, A.M., and Constantinou, M.C., (1991), "Nonlinear dynamic analysis of base 3D base isolated structures," *Journal of Structural Engineering,* 117:2035-2054.

36. Nagarajaiah, S., Reinhorn, A.M., and Constantinou, M.C., (1992), "Experimental study of sliding isolated structures with uplift restraint," *Journal of Structural Engineering,* 118(6):1666-1682.

37. Nagarajaiah, S., Reinhorn, A.M., and Constantinou, M.C., (1993), "Torsional coupling in sliding base isolated structures," *Journal of Structural Engineering,* 119: 130-149.

38. Nagarajaiah, S., Reinhorn, A.M., and Constantinou, M.C., (1998), "Nonlinear dynamic analysis of three-dimensional base isolated structures (3d-basis)," Technical Report NCEER-89-0019, National Center of Earthquake Engineering Research, SUNY, Buffalo.

39. Nagarajaiah, S. and K. Ferrell, (1999), "Stability of elastomeric seismic isolation bearings," *Journal of Structural Engineering,* 125(9): 946-954.

40. Nagarajaiah, S. and S. Xiahong, (2000), "Response of base-isolated USC Hospital Building in Northridge Earthquake," *Journal of Structural Engineering,* 126(10):1177-1186.

41. Oka, N.A., (2000), "Nonlinear dynamic analysis of an asymmetric structure fitted with semi-active hydraulic devices", M.Sc. Thesis, Duke University.

42. Onoda, J., Oh, H.U., Minesugi, K., (1997), "Semi-active vibration suppression of truss structures by electrorheological fluid," *ACTA Astronautica,* 40(11):771-779.

43. Pan, T.C. and J.M., Kelly (1983), "Seismic response of torsionally coupled base isolated building," *Earthquake Engineering and Structural Dynamics,* 11: 749-770.

44. Patten, W.N., Mo., J., Kuehn, M.J., and Lee, J., (1998), "A primer on design of semi-active vibration absorbers," *Journal of Engineering Mechanics,* 124(1):61-68.

45. Skinner, R.I., Robinson, W.H., McVerry, G.H., (1993), "An introduction to seismic isolation," *John Wiley.*

46. Soong, T.T., (1990), "Active structural control: Theory and Practice," *Longman,*

47. Spencer Jr., B.F., Dyke, S.J., and Sain, M.K., (1996), "Magnetorheological dampers: a new approach to seismic protection of structures," *Proc. of Conf. on Decision and Control,* pp. 676-681.

48. Symans, M.D. and M.C., Constantinou, (1997a), "Seismic testing of a building structure with a semi-active fluid damper control sytem," *Earthquake Engineering and Structural Dynamics,* 26: 759-777.

49. Symans, M.D. and M.C., Constantinou, (1997b), "Experimental testing and analytical modeling of semi-active fluid dampers for seismic protection", *Journal of Intelligent Material Systems and Structures,* 8(8): 644-657.

50. Symans, M.D. and M.C., Constantinou, (1999), "Semi-active control systems for seismic protection of structures: a state of the art view", *Engineering Structures,* 21(6): 469-487.

51. Tyler, R.G. (1977), "Dynamic tests on PTFE sliding layers under earthquake conditions", *Bulletin of the New Zealand National Society of Earthquake Engineering,* 10(3).

52. Wang, Y.P., Chung, L.L., and Liao, W.H., (1998), "Seismic response analysis of bridges isolated with friction pendulum bearings," *Earthquake Engineering and Structural Dynamics,* 27:1069-1093.

53. Yang, J.N., Kim, J.H., and Anil, K.A., (2000), "Resetting semiactive stiffness damper for seismic response control," *Journal of Structural Engineering,* 126912):1427-1433.

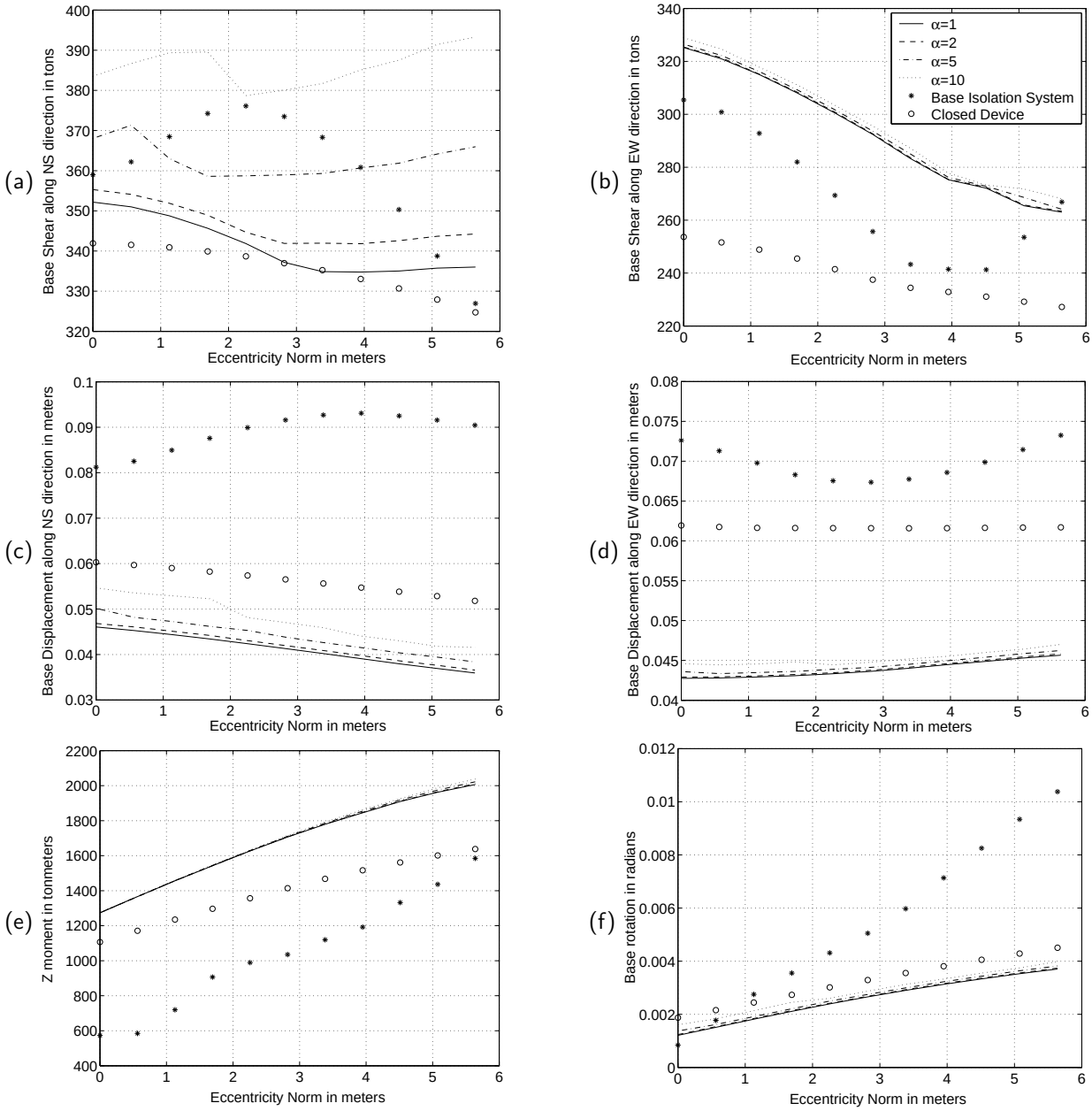

Figure 4: Comparison of the isolation drift (a)&(b), base shears (c)&(d), torsional rotation and moment (e)&(f) between the LRB system, the LRB-SAVD system with variation in α and the LRB-VD system for El Centro.

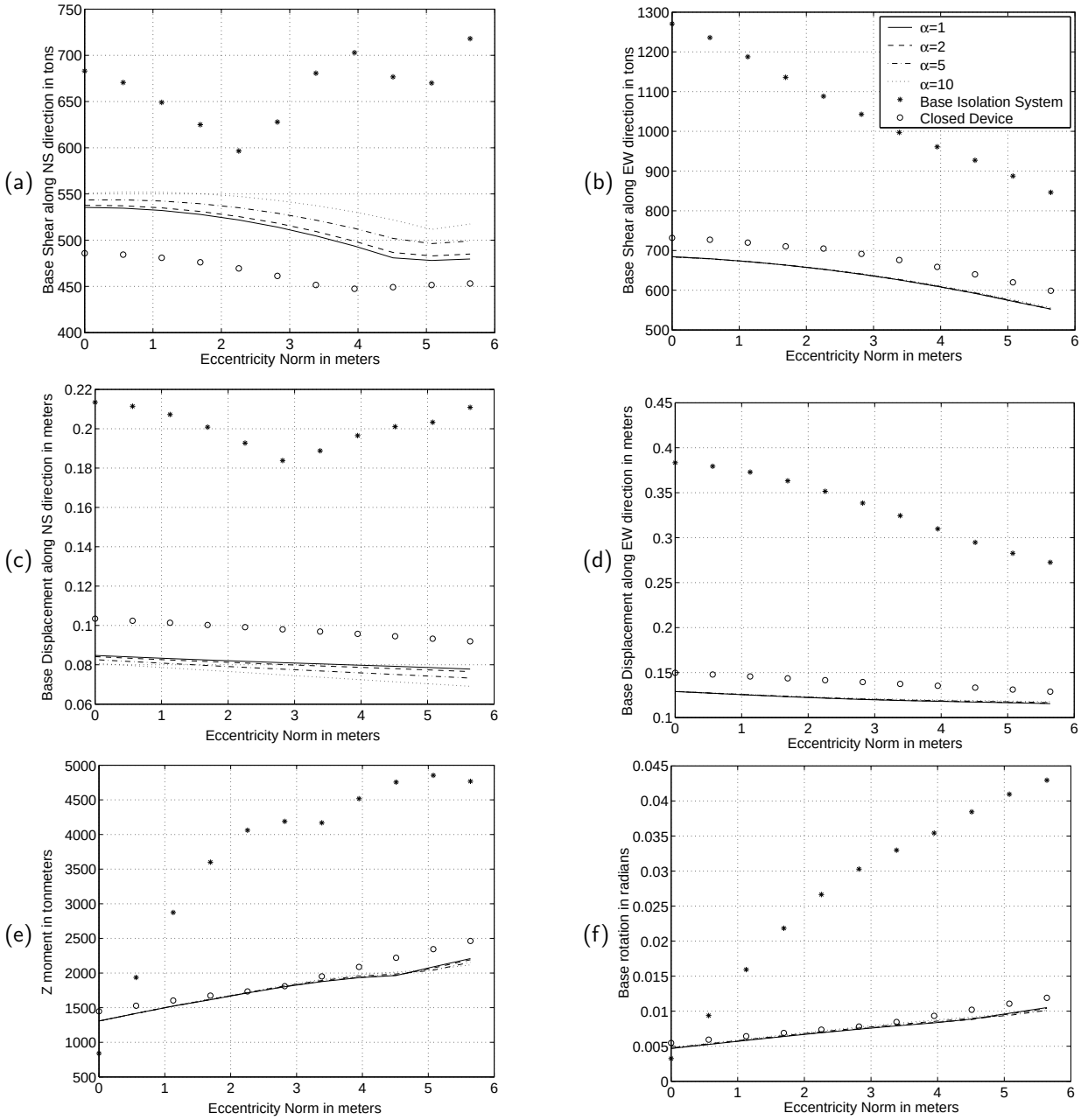

Figure 5: Comparison of the isolation drift (a)&(b), base shears (c)&(d), torsional rotation and moment (e)&(f) between the LRB system, the LRB-SAVD system with variation in α and the LRB-VD system for Meloland.

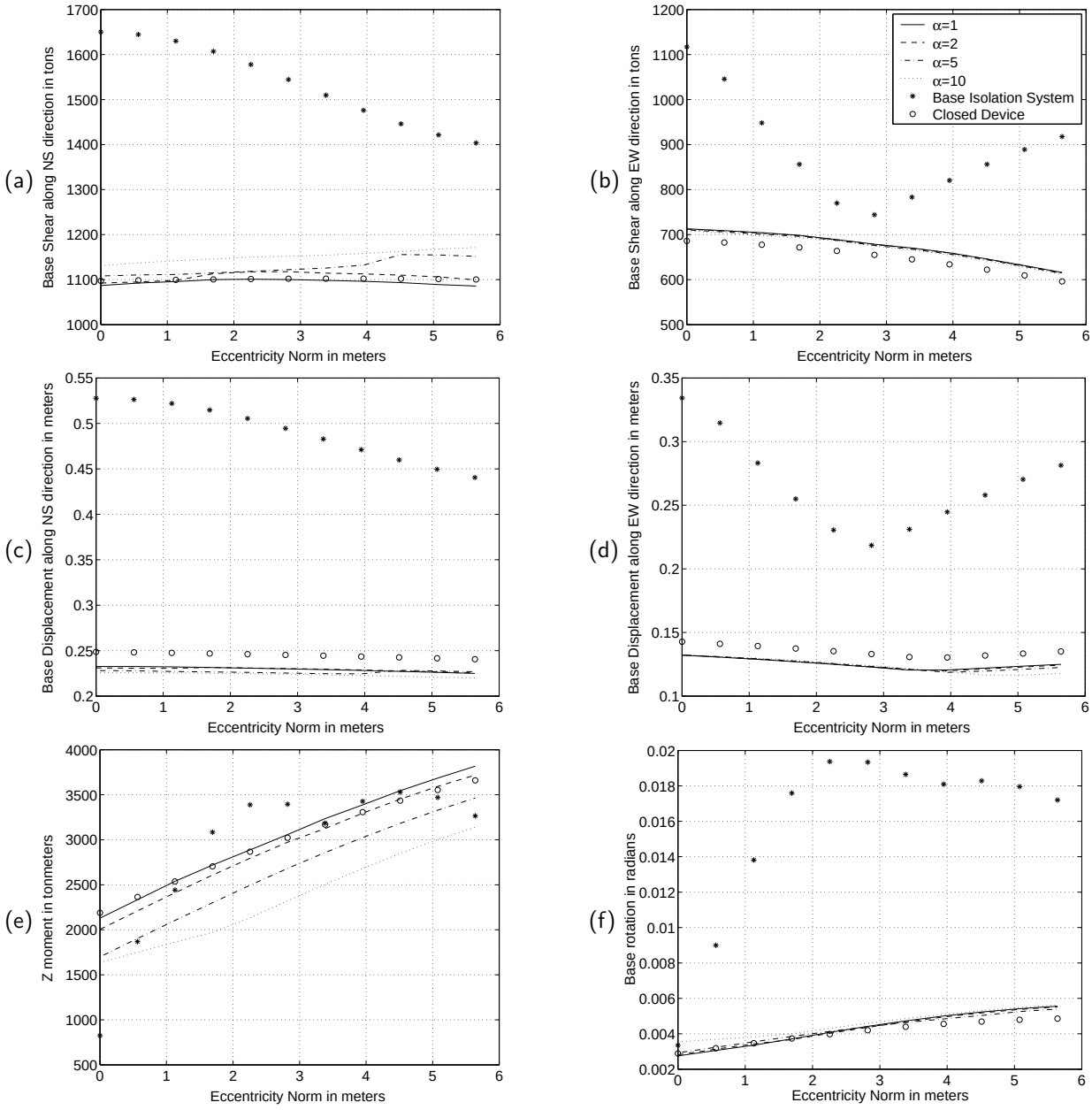

Figure 6: Comparison of the isolation drift (a)&(b), base shears (c)&(d), torsional rotation and moment (e)&(f) between the LRB system, the LRB-SAVD system with variation in α and the LRB-VD system for Sylmar.